Cholesterol Flip−Flop: Insights from Free Energy Simulation Studies

ARTICLE *in* THE JOURNAL OF PHYSICAL CHEMISTRY B · OCTOBER 2010

Impact Factor: 3.3 · DOI: 10.1021/jp108166k · Source: PubMed

5 AUTHORS, INCLUDING:

Sunhwan Jo
Argonne National Laboratory
35 PUBLICATIONS **1,212** CITATIONS
SEE PROFILE

Huan Rui
University of Chicago
23 PUBLICATIONS **292** CITATIONS
SEE PROFILE

Jeffery Klauda
University of Maryland, College Park
93 PUBLICATIONS **2,564** CITATIONS
SEE PROFILE

Cholesterol Flip-Flop: Insights from Free Energy Simulation Studies

Sunhwan Jo,[†,‡] Huan Rui,[†,§] Joseph B. Lim,[||] Jeffery B. Klauda,[||] and Wonpil Im*[,‡,§]

Department of Molecular Biosciences and Center for Bioinformatics, The University of Kansas, 2030 Becker Drive, Lawrence, Kansas 66047, United States, and Department of Chemical and Biomolecular Engineering, The University of Maryland, College Park, Maryland 20742, United States

Received: September 7, 2010

The mechanism of lipid flip-flop motion is important for maintaining the asymmetric distribution of lipids in a biological membrane. To explore the energetics and mechanism of passive cholesterol flip-flop and its dependence on chain saturation, we performed two-dimensional umbrella sampling simulations in DPPC, POPC, and DAPC (dipalmitoyl-, palmitoyloleoyl-, and diarachidonylphosphatidylcholine) and used the string method to identify the most probable flip-flop paths based on the two-dimensional free energy maps. The resulting paths indicate that cholesterol prefers to tilt first and then move to the bilayer center where the free energy barrier exists. The barrier is lower in DAPC than in DPPC or POPC, and the calculated flip-flop rates show that cholesterol flip-flop in a poly-unsaturated bilayer is faster than in more saturated bilayers. The free energy barrier results from the unfavorable enthalpic contribution arising from cholesterol−water/lipid interactions and the favorable entropic contribution due to increased lipid dynamics. While the cholesterol−water interaction has similar contributions to the barrier due to desolvation of the cholesterol hydroxyl group in all lipids, the cholesterol−lipid interaction has a much lower barrier in DAPC than in DPPC or POPC, resulting in the lower free energy barrier in DAPC.

1. Introduction

The movement of lipids (including sterols) within a membrane consists of either lateral diffusion or flip-flop between leaflets. In general, lipid lateral diffusion (in homogeneous bilayers or in and out of different domains in heterogeneous bilayers) is much faster than the rate of flip-flop and is well-described by experiments[1] and simulations.[2,3] The concentrations of phospholipids are different between the inner and outer leaflets of cellular membranes and vary in different types of membranes.[4] It has been suggested that cholesterol may have different concentrations in different leaflets of plasma membranes.[5,6] The mechanism for lipid exchange between leaflets can involve either passive exchange or protein-assisted movement by flop- and flippases.[4] The present study focuses on passive exchange of cholesterol using computer simulations and free energy calculations.

Recent neutron scattering experiments showed that a significant amount of cholesterol exists in a parallel orientation (to the membrane surface) at the center of bilayers composed of poly-unsaturated lipids, such as DAPC (diarachidonylphosphatidylcholine), whereas such an orientation is absent in POPC (palmitoyloleoylphosphatidylcholine) and DPPC (dipalmitoylphosphatidylcholine) bilayers.[7,8] These phenomena have been further clarified by Kučerka et al.[9] with mixed phospholipid membranes; cholesterol reverts back to its standard perpendicular orientation (to the membrane surface) when DAPC is mixed with >50% POPC or with only >5% DMPC. These observations suggest that the rate of cholesterol flip-flop is enhanced in bilayers composed of poly-unsaturated lipids compared to those with more saturated chains.

Recently, molecular dynamics (MD) and free energy simulations have been used to further describe cholesterol's preference to a parallel orientation in DAPC[10] and cholesterol leaflet flip-flop[11] or transfer to/from the water phase.[12] Coarse-grained MD simulations of cholesterol in DAPC resulted in equilibrium sterol structures parallel to the membrane surface at the center of the bilayer, but cholesterol in a POPC membrane was in the standard perpendicular orientation.[10] While these results agree with the aforementioned experiments qualitatively, the amount of sterol at the center of the bilayer is not in quantitative agreement. Moreover, simulations with an all-atom force field did not result in stable cholesterol orientations at the center of the bilayer (see the Supporting Information in ref 10). Zhang et al. have used umbrella sampling MD simulations to describe the potentials of the mean force (PMF) of moving cholesterol from POPC or sphingomyelin bilayers to the water phase.[12] Preference for sphingomyelin-containing bilayers is observed as expected, but the detailed analysis showed that this resulted from a favorable change in lipid−lipid interactions over cholesterol−lipid interactions, which was unexpected. Bennett et al. have used similar approaches and calculated the PMFs of cholesterol transfer from water to various lipid bilayers in both coarse-grained and (united) all-atom models.[11] The cholesterol flip-flop rates estimated on the basis of the PMFs were a sub-microsecond time scale in DAPC and the second range in DPPC with high cholesterol concentration.[11]

To further explore the energetics and mechanism of cholesterol flip-flop and its dependence on chain saturation, we used both two-dimensional (2D) umbrella sampling free energy and standard MD simulations of cholesterol in DPPC, POPC, and DAPC lipid bilayers. It should be noted that the reaction coordinates in the umbrella sampling simulations are the tilt angle of the rigid cholesterol ring and its center of mass along the *Z*-axis in our work, while the aforementioned free energy simulations used only the *Z*-axis as the reaction coordinate. We also employed the string method[13] to identify the most probable flip-flop paths based on the 2D-PMF surface. To verify the PMF results and estimate the flip-flop kinetics, we performed a set of standard MD simulations of cholesterol starting from its parallel orientation at the center of each bilayer. In the following section, the simulation details such as restraint potentials, system

* To whom correspondence should be addressed. Tel.:785-864-1993. E-mail:wonpil@ku.edu.
[†] Both authors contributed equally to this work.
[‡] Department of Molecular Biosciences, The University of Kansas.
[§] Center for Bioinformatics, The University of Kansas.
[||] The University of Maryland.

10.1021/jp108166k
Published on Web 10/05/2010

building, umbrella sampling simulation parameters, and path determination using the string method are described in detail. The results are then given and discussed.

2. Methods

Methods is divided into three subsections. Section 2.1 describes the 2D umbrella sampling MD simulations to calculate the 2D-PMF as a function of the tilt angle (τ) of the rigid cholesterol ring and its center of mass along the *Z*-axis (Z_{CM}) in DPPC, POPC, and DAPC lipid membranes. Section 2.2 describes the standard MD simulations to further verify the PMF results and estimate the passive cholesterol flip-flop kinetics. Section 2.3 describes the modified string method to calculate the most probable flip-flop paths on the resulting 2D-PMF.

2.1. Umbrella Sampling MD Simulation. ***Tilt Restraint Potential.*** We used a simple harmonic function for the tilt restraint potential,

$$U_\tau(\mathbf{R}) = \frac{1}{2}k_\tau(\tau(\mathbf{R}) - \tau_0)^2 \quad (1)$$

where $\mathbf{R}$ represents a set of selected atoms, i.e., $\mathbf{R} \equiv \{\mathbf{r}_\alpha\}$, used to define the principal axis of the molecule of interest, k_τ is the force constant, and τ_0 is the target tilt angle. The instantaneous tilt angle, τ, is defined by the angle between the principal axis ($\hat{a}$) of the molecule of interest and an arbitrary axis ($\hat{p}$),

$$\tau = \cos^{-1}(\hat{a}\cdot\hat{p}) \quad (2)$$

where $|\hat{a}| = |\hat{p}| = 1$. The force acting on an atom α due to the deviation of τ from τ_0 becomes

$$\frac{\partial U_\tau}{\partial \mathbf{r}_\alpha} = -k_\tau(\tau - \tau_0)\frac{1}{\sin\tau}\frac{\partial \cos\tau}{\partial \mathbf{r}_\alpha} \quad (3)$$

where the derivative of cos τ with respect to $\mathbf{r}_\alpha$ is given by

$$\frac{\partial \cos\tau}{\partial \mathbf{r}_\alpha} = \frac{\partial}{\partial \mathbf{r}_\alpha}\left(\frac{\hat{a}\cdot\hat{p}}{|\hat{a}||\hat{p}|}\right) = \hat{p}\,\frac{\partial \hat{a}}{\partial \mathbf{r}_\alpha} - a^2\hat{p}\,\frac{\partial \hat{a}}{\partial \mathbf{r}_\alpha} \quad (4)$$

The derivative of the eigenvector components, $\partial\hat{a}_n/\partial\mathbf{r}_\alpha$ ($n = x, y, z$), is well-described in ref 14.

Umbrella Sampling MD Simulations. Using the Membrane Builder module[15,16] in CHARMM-GUI (http://www.charmm-gui.org),[17] each lipid system was built with two cholesterol molecules (A and B) and 98 lipid molecules (one cholesterol and 49 lipid molecules in each leaflet) in 0.15 M KCl solution. The initial system sizes and the number of each component are given in Supporting InformationTable S1. Two cholesterol molecules in each lipid system were moved to $X = Y = +14$ Å and $X = Y = -14$ Å, respectively, to minimize their interactions during the flip-flop event. The *X* and *Y* of each cholesterol ring's center of mass were restrained to $X = Y = +14$ Å and $X = Y = -14$ Å throughout the simulations. To relax the uncorrelated initial systems, 350 ps equilibration was performed with tilt restraint potentials for $\tau_A = 0°$ and $\tau_B = 180°$. It should be noted that the ring atoms of cholesterol and the *Z*-axis were used to define the principal axis ($\hat{a}$) and the arbitrary axis ($\hat{p}$) in eq 2, respectively.

To perform umbrella sampling MD simulations as a function of the tilt angle of the rigid cholesterol ring and its center of mass along the *Z*-axis (Z_{CM}), an initial structure at each window was first generated by translating $Z_{CM,A}$ (of cholesterol A) from +14 to −14 Å by 2 Å every 50 ps and then by tilting the cholesterol rings from $\tau_A = 0°$ to $\tau_A = 90°$ (on the *XZ* plane) by 5° every 50 ps for each Z_{CM} position, resulting in 285 windows (Figure 1 and Supporting Information Figures S1−S3 for the snapshots of a few selected windows in each lipid). At the same time, cholesterol B moved/tilted in an opposite orientation; i.e., $Z_{CM,B} = -Z_{CM,A}$ and $\tau_B = 180° - \tau_A$. Such a system setup allowed us not only to increase sampling by simulating two independent cholesterol molecules but also to cover the entire cholesterol flip-flop path. It should be noted that the cholesterol ring can rotate along its principal axis, although its tilt angle was restrained to a specific value in each window on the *XZ* plane. For each window, we first ran 2 ns umbrella sampling simulations, calculated the 2D-PMFs (see WHAM calculations below), and identified the regions with prohibitively high energy barriers ($Z_{CM} \le -6$ Å and $\tau \le 70°$ in Supporting Information Figure S4). Those regions were excluded to reduce the number of windows, and we continued the simulations in the remaining 210 windows to 7 (DPPC and POPC) and 8 ns (DAPC) for better PMF convergence. We used the last 5 ns for the final PMF calculations and trajectory analyses. The force constants of τ and Z_{CM} restraint potentials were set to 1000 kcal/(mol·rad^2) and 1 kcal/(mol·Å^2) for both equilibration and production.

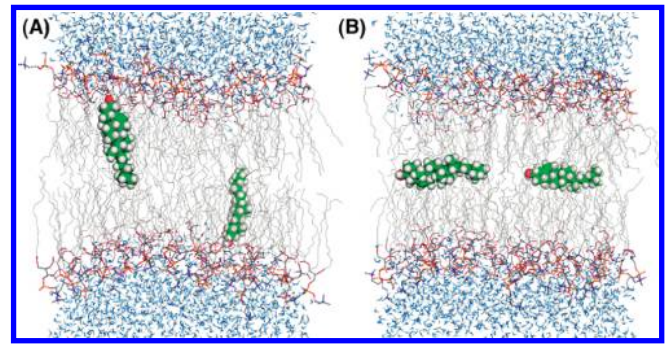

Figure 1. Cholesterol flip-flop simulation systems in DPPC. There are two cholesterol molecules, A (left) and B (right), in each system. (A) $\tau_A = 15°$, $\tau_B = 165°$, $Z_{CM,A} = 10$ Å, and $Z_{CM,B} = -10$ Å. (B) $\tau_A = \tau_B = 90°$, and $Z_{CM,A} = Z_{CM,B} = 0$ Å.

All calculations were performed in the *NPγT* ($\gamma = 10$ dyn/cm) ensemble[18,19] at 323.15 (DPPC) and 303.15 K (POPC and DAPC) using the biomolecular simulation program CHARMM[20] with the all-atom C27r parameter set[21,22] and the modified TIP3P water model.[23,24] A time step of 2 fs was used for the *NPγT* dynamics with the SHAKE algorithm.[25] We used the same options for nonbonded interactions as in the input scripts provided by the CHARMM-GUI Membrane Builder;[15,16] the van der Waals interactions were smoothly switched off at 11−12 Å by a force switching function,[26,27] and electrostatic interactions were calculated using the particle-mesh Ewald (PME) method with a mesh size of about 1 Å for fast Fourier transformation, $\kappa = 0.34$ Å^{-1}, and a sixth-order B-spline interpolation.[28]

WHAM Calculations. The biased τ and Z_{CM} distributions of cholesterols A and B from the umbrella sampling simulations were first symmetrized and unbiased by the WHAM[29] analysis to construct the 2D-PMFs. The free energy was calculated for every 1° and 0.5 Å along τ and Z_{CM} with an energy tolerance of 10^{-5} kcal/mol.

2.2. Standard MD Simulations. Starting from the last snapshot of the window corresponding to the parallel cholesterol orientation at the bilayer center (i.e., $Z_{CM} = 0$ and $\tau = 90°$), we performed 50 independent standard MD simulations (without

restraints) with different initial velocity assignments in each bilayer. Each simulation ran for 12 ns with the aforementioned simulation options and ensemble ($NP\gamma T$), and the return time to the preferred thermally accessible orientations was measured for 100 cholesterols in each bilayer (n.b., each system has two cholesterol molecules).

2.3. Flip-Flop Path Calculation. ***Generating the Initial Pathway.*** A pathway between two distinctive states of cholesterol is denoted by a fixed number of images, and every image corresponds to a point on the 2D-PMF surface. The initial pathway was generated by distributing 50 images uniformly along the line connecting (0°, +14 Å) and (180°, −14 Å) in the PMF map, which represent cholesterol orientations with $\tau = 0°$, $Z_{CM} = +14$ Å and $\tau = 180°$, $Z_{CM} = -14$ Å, respectively. The images were numbered from 0 to 49. The initial pathways for cholesterol flip-flop are shown on the 2D-PMF in DPPC, POPC and DAPC (Supporting Information Figure S5).

Evolving the Pathway by a Modified String Method. We modified the string method[13] to evolve the initial pathway to the most probable pathway. Instead of Brownian dynamics simulations used in the original string method, we applied Monte Carlo (MC) simulations to propagate the images on the initial pathway. A group of 20000 MC iterations was sufficient to obtain the converged final pathway. For efficient energy evaluations during MC simulations, we mapped the 2D-PMF onto a 200 × 200 grid with grid spacing of 0.9° (h_τ) along τ and 0.14 Å (h_Z) along Z_{CM}, respectively. The modified string method involved the following three steps:

(1) A random movement with $-h_\tau \le d\tau \le +h_\tau$ and $-h_Z \le dZ_{CM} \le +h_Z$ was made for each of the 48 images along the pathway. Note that we fixed the first and last images. We evaluated the free energy associated with each move, and the position of each image was then updated on the basis of the Metropolis criteria.[30]

(2) The newly generated pathway was smoothed by

$$\mathbf{r}_k^{\text{smooth}} = (1 - s)\mathbf{r}_k + \frac{s}{2}(\mathbf{r}_{k-1} + \mathbf{r}_{k+1}) \tag{5}$$

where $\mathbf{r}_k$ and $\mathbf{r}_k^{\text{smooth}}$ represent the position of the kth image ($k = 1, 2, 3, ..., 48$) on the grid before and after smoothing. s is the smoothing factor ranging from 0 to 1. In the present study, s was empirically chosen to be 0.75.

(3) After calculating the total length of the pathway, $L(k)$ ($k = 49$), and a desired length of the pathway up to the mth image, $S(m)$, we reparametrized the pathway by distributing the images uniformly along the smoothed pathway. This process was performed by

$$\begin{aligned} &L(k-1) \le S(m) < L(k) \\ &\mathbf{r}_m^{\text{repar}} = \frac{L(k) - S(m)}{L(k) - L(k-1)}\mathbf{r}_{k-1}^{\text{smooth}} + \frac{S(m) - L(k-1)}{L(k) - L(k-1)}\mathbf{r}_k^{\text{smooth}} \end{aligned} \tag{6}$$

where $L(k)$ is the length between image 0 and k along the smoothened pathway. $\mathbf{r}_k^{\text{repar}}$ is the position of the kth image on the grid after reparametrization.

These three steps were iterated 20000 times to achieve the convergence of the flip-flop transition pathway. Supporting Information Movies M1−M3 show the evolution of the pathways in the DPPC, POPC, and DAPC bilayers.

Identifying the Average Transition Path Ensemble. We performed 1000 independent MC runs (each with 20000 MC steps) each starting from the initial path to obtain a statistically meaningful average pathway. Since the 2D-PMF profile was symmetric around $\tau = 90°$ and $Z_{CM} = 0$ Å, any individual pathway with more than 25 images with $\tau < 90°$ was subjected to a symmetry operation:

$$\begin{bmatrix} \tau'_k \\ Z'_k \end{bmatrix} = \begin{bmatrix} -1 & 0 \\ 0 & -1 \end{bmatrix} \begin{bmatrix} \tau_k \\ Z_k - 14 \end{bmatrix} + \begin{bmatrix} 180 \\ 14 \end{bmatrix} \tag{7}$$

where τ_k, Z_k and τ'_k, Z'_k are the τ and Z_{CM} of the kth image before and after the symmetry operation, respectively. The kth images from all 1000 pathways after the symmetry operation were plotted in the τ and Z_{CM} space; the center of the distribution was chosen as the average position of the kth image (τ_k^{av}, Z_k^{av}). The average pathway can then be defined by the set of averaged images (Supporting Information Figure S6).

The difference between the individual and the average pathways was calculated by

$$d^{(i)} = \frac{1}{N}\sqrt{\sum_{k=0}^{49}[(\tau_k^{(i)} - \tau_k^{av})^2 + (Z_k^{(i)} - Z_k^{av})^2]} \tag{8}$$

where N is the total number of images ($N = 50$) and i is the index number of independent MC runs ($i = 1, 2, 3, ..., 1000$). The set of pathways with $d^{(i)} \le 0.3$ was then defined as the average pathway ensemble, on the basis of which the averaged PMF and interaction energies were calculated. The average pathway ensembles in DPPC, POPC, and DAPC are also shown in Figure S6.

3. Results and Discussion

Cholesterol Flip-Flop Pathways. Figure 2 shows the 2D-PMFs as a function of the tilt angle (τ) of the rigid cholesterol ring and its center of mass along the Z-axis (Z_{CM}) in DPPC, POPC, and DAPC bilayers. While the thermally accessible regions of cholesterol orientations are broad for each bilayer, the minimum-PMF tilt regions (τ_{min} within ±0.1 kcal/mol) are found to be 17 ± 5° (DPPC), 22 ± 5° (POPC), and 28 ± 5° (DAPC), respectively. The order in τ_{min} correlates well with the bilayer fluidity, which increases as the acyl chain unsaturation increases. The standard MD simulations starting in the parallel cholesterol orientation (see Methods section 2.2) also show broad τ distributions around τ_{min} after they returned to the thermally accessible cholesterol orientation (Supporting Information Figures S7 and S8). As we previously showed in the yeast-like membrane systems,[15] the cholesterol tilt does respond to changes in the bilayer properties; i.e., cholesterol tilts less in bilayers with more saturated lipids.

The PMFs clearly show that the passive cholesterol flip-flop is energetically unfavorable. As described in Methods section 2.3 and shown in Movies M1−M3, we used the modified string method[13] to determine the most probable flip-flop paths on the 2D-PMFs. The resulting paths are shown on the 2D-PMF surfaces in Figure 2, and the cholesterol orientations along the paths are shown in Supporting Information Figure S9. Cholesterol adapts an orientation parallel to the membrane surface near the bilayer center ($|Z_{CM}| < 5$ Å) along the flip-flop path. Interestingly, the paths clearly indicate that, before cholesterol reaches near the bilayer center, the most prevailing change in its orientation is in the tilt angle. In other words, cholesterol prefers to tilt first and move to the bilayer center where the

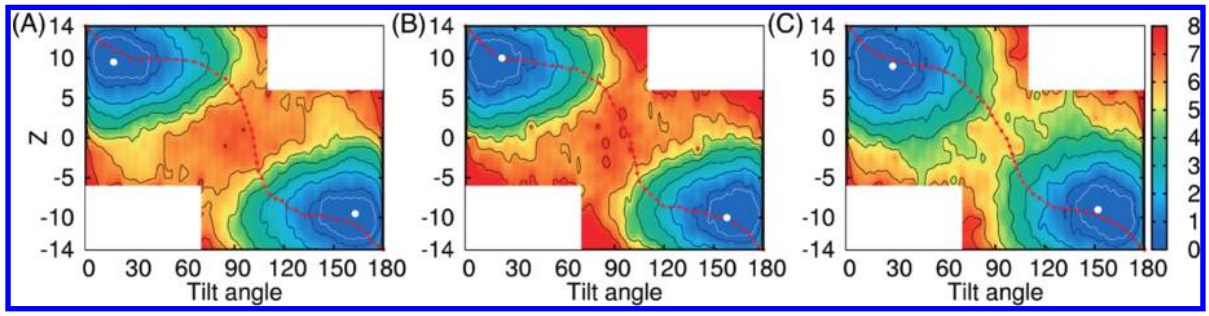

Figure 2. 2D-PMFs (kcal/mol) in (A) DPPC, (B) POPC, and (C) DAPC bilayers. The black lines are drawn every 1 kcal/mol, and the white lines represent the thermally accessible regions from the PMF minimum (white dot). The most probable flip-flop path is shown in red.

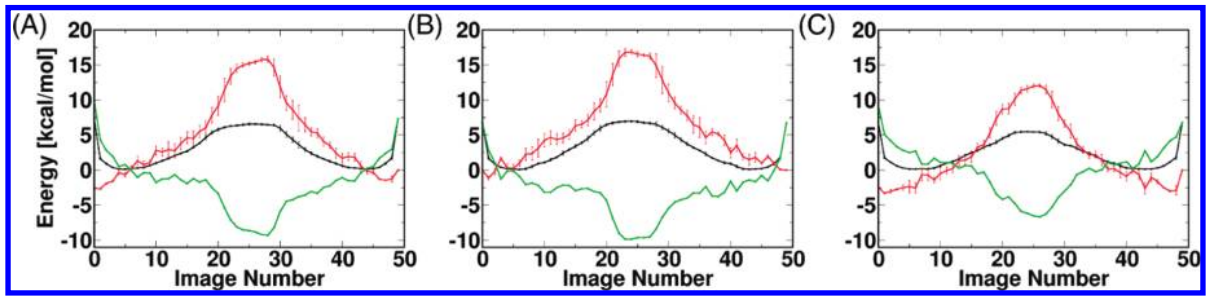

Figure 3. Free energy profile (black) along the path and its decomposition into enthalpic (i.e., interaction energy, red) and entropic (green) contributions in (A) DPPC, (B) POPC, and (C) DAPC bilayers.

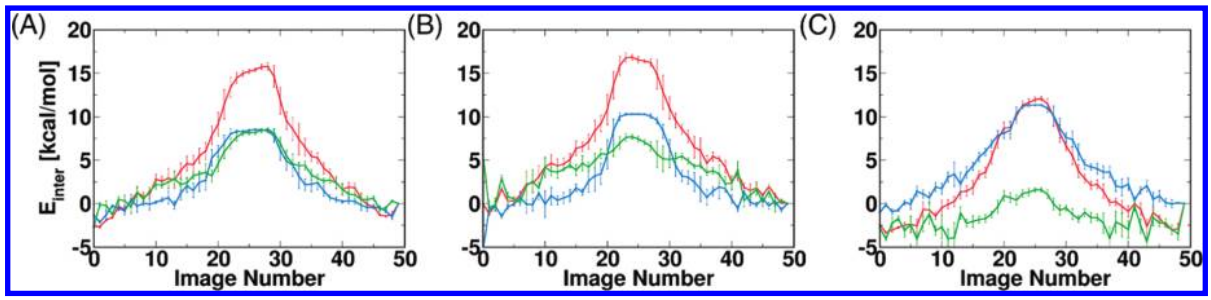

Figure 4. Decomposition of the interaction energy profile (red) along the path into cholesterol−lipid (green) and cholesterol−water (blue) interaction energies in (A) DPPC, (B) POPC, and (C) DAPC bilayers.

TABLE 1: Thermodynamics and Kinetics of Cholesterol Flip-Flop in DPPC, POPC, and DAPC

system	temperature[a] (K)	ΔG^b (kcal/mol)	$t_d{}^c$ (ns)	$k_d{}^d$ (s^{-1})	$k_f{}^e$ (s^{-1})	$k_{flip}{}^f$ (s^{-1})
DPPC	323.15	6.6 ± 0.1	0.5 to 6.4	1.6×10^8 to 2.0×10^9	2.5×10^3 to 3.1×10^4	1.2×10^3 to 1.6×10^4
POPC	303.15	7.0 ± 0.1	1.0 to 8.5	1.2×10^8 to 1.0×10^9	9.5×10^2 to 8.0×10^3	4.8×10^2 to 4.0×10^3
DAPC	303.15	5.4 ± 0.1	0.7 to 8.8	1.1×10^8 to 1.4×10^9	1.3×10^4 to 1.6×10^5	6.0×10^5 to 8.0×10^6

[a] Simulation temperature. [b] Free energy barrier along the most probable flip-flop path (Figure 3). [c] Estimated time ranges for cholesterol to move from the parallel cholesterol orientation in the bilayer center to the preferred orientation (i.e., the thermally accessible orientation) in the standard MD simulations. [d] $k_d = 1/t_d$. [e] Calculated rate for cholesterol to move from the preferred orientation to the parallel cholesterol orientation in the bilayer center: $k_f = k_d \exp(-\Delta G/k_B T)$.[11] [f] Calculated rate for cholesterol flip-flop: $k_{flip} = 1/(k_f{}^{-1} + k_d{}^{-1}) \times 1/2 \approx k_f/2$.[11]

free energy barrier exists. In fact, a short-lived parallel orientation even at $|Z_{CM}| > 5$ Å was observed in the MD simulations of the yeast-like membrane systems with a high concentration of unsaturated chains,[15] which is also consistent with the 2D-PMF (Figure 2) and standard MD simulation (Figure S8) results.

Thermodynamics and Kinetics of Cholesterol Flip-Flop. The free energy changes along the paths determined by the modified string method are shown in Figure 3. The energy barriers near each bilayer center are 6.6 ± 0.1 (DPPC), 7.0 ± 0.1 (POPC), and 5.4 ± 0.1 kcal/mol (DAPC). Consistent with the 2D-PMFs, most cholesterol in the standard MD simulations moved from the initial parallel orientation to the thermally accessible cholesterol orientations (see Figures S8 and S10). Although the PMF in DAPC shows a lower barrier than those in DPPC and POPC, we did not observe the free energy minimum in the bilayer center with the C27r force field (FF).[31] Previous coarse-grained (CG) simulations did result in such parallel orientations,[10] but the percentage of cholesterol in this orientation was significantly less than what was suggested by the neutron scattering experiment.[8] Moreover, such parallel orientations were not observed in previous all-atom simulations.[10] This result suggests that the C27r and other all-atom FFs may require further optimization to capture a preference for parallel cholesterol at the center of poly-unsaturated lipid bilayers (see Conclusions). Nonetheless, it is still instructive to extract the kinetic information of cholesterol flip-flop rates on the basis of our 2D-PMFs and the standard MD simulations and compare them with the recently published results based on 1D-PMF along the *Z*-axis and a united atom model.[11]

Similar to Table 1 in ref 11, we summarize all thermodynamic and kinetic information in Table 1. First, the free energy barriers (ΔG) in DPPC and DAPC are 6.6 and 5.4 kcal/mol in our 2D-

PMFs, and 5.7 and 4.3 kcal/mol in their 1D-PMFs [n.b., the simulation temperatures in DAPC are different: 303 K in the current study and 323 K in ref 11]. Second, the standard MD simulations were used to estimate time ranges for cholesterol to move from the parallel orientation in the bilayer center to the preferred thermally accessible orientation (t_d in Table 1). As shown in Supporting Information Figure S11, the t_d distribution is broad within the simulation time and is not statistically well-defined even with 50 independent runs in each bilayer. Given the statistical errors and the stochastic nature of the returning events, we estimated a range of t_d by neglecting the five highest and five lowest t_d, and the values are given in Table 1. Although such estimates are not rigorous, estimating the ranges of t_d is significant because the corresponding rate k_d, which is $1/t_d$, is a prefactor necessary to determine a rate (k_f) for cholesterol to move from the preferred orientation to the parallel orientation in the bilayer center: $k_f = k_d \exp(\Delta G/k_B T)$. Interestingly, t_d appears to be more dependent on temperature than the barrier itself in the current simulations (Figure S11); the t_d distribution shows smaller t_d for DPPC compared to POPC although their barriers are similar, while t_d is similar for POPC and DAPC bilayers although their barriers are different. Third, the cholesterol flip-flop rates (k_{flip}) can be estimated on the basis of k_d and k_f,[11]

$$k_{flip} = \frac{1}{(k_f^{-1} + k_d^{-1})} \times \frac{1}{2} \quad (9)$$

When $k_f^{-1} >> k_d^{-1}$, which is the current case, $k_{flip} \approx k_f/2$, indicating that, given the energy barrier, the movement from the preferred cholesterol orientation to the parallel orientation at the bilayer center is the rate-determining step, and a cholesterol at the bilayer center has the equal probability to return back to the original orientation or to flip-flop into the other leaflet. The estimated k_{flip} are 1.2×10^3 to 1.6×10^4 s^{-1} (DPPC) and 6.0×10^5 to 8.0×10^6 s^{-1} (DAPC) in our calculations, and 1.2×10^4 to 6.6×10^5 s^{-1} (DPPC) and 5.2×10^5 to 3.7×10^6 s^{-1} (DAPC) from ref 11. Given the differences in computational approaches and models, the agreement between our results and their results is reasonable. Intuitively, these rates appear to be very fast. There are no experimental data with which we can directly compare our results, and the experimental flip-flop rates vary significantly,[32,33] but a recent experimental study suggested that the flip-flop rate of cholesterol in human red cell is >1 s^{-1}.[34]

Free Energy Decomposition. To explore the microscopic forces governing the energetics of cholesterol flip-flop, we calculated the interaction energies between cholesterol and water/lipid molecules along the paths (Figure 4). Clearly, desolvation of the cholesterol hydroxyl group is attributed to the energy barrier of the cholesterol−water interaction along the path. Interestingly, however, the energy barrier due to desolvation increases in the order of DPPC (8.5 kcal/mol), POPC (10.3 kcal/mol), and DAPC (11.4 kcal/mol), suggesting that the desolvation penalty during cholesterol flip-flop is slightly more in unsaturated lipids. This arises from the fact that more water molecules are deprived from interacting with the cholesterol hydroxyl group during sterol flip-flop in the bilayers containing more unsaturated lipids, because their membrane thickness with cholesterol in its standard perpendicular orientation is thinner than that of more saturated lipid bilayers (Figure 5). In other words, the cholesterol hydroxyl group in the minimum-PMF orientation has more surrounding water molecules in more unsaturated lipid bilayers, and there are no water molecules surrounding the cholesterol hydroxyl group at the bilayer center regardless of lipid types, which results in more unfavorable cholesterol−water interaction along the flip-flop path in more unsaturated lipid bilayers. The cholesterol−lipid interaction has an energy barrier due to reduction of favorable cholesterol−lipid interactions along the path in DPPC and POPC. In other words, DPPC and POPC molecules are well-packed around cholesterol with the preferred orientation, while the packing is not optimal when cholesterol is in a parallel orientation at the bilayer center. However, such reduction of cholesterol−lipid interaction along the path is not significant in DAPC, and thus the total interaction energy barrier is significantly lower in DAPC (Figure 4).

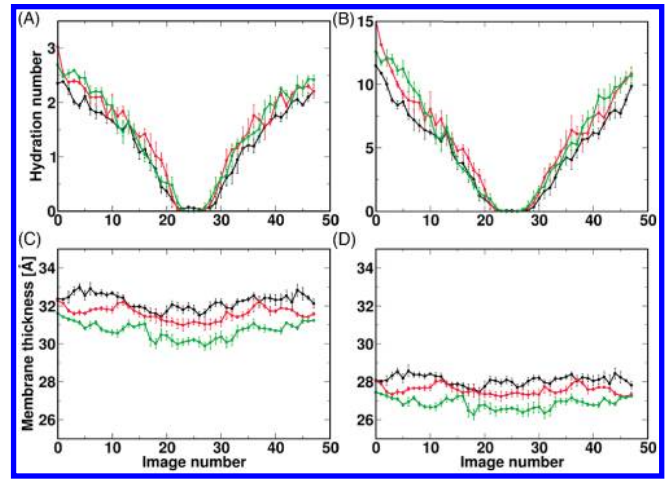

Figure 5. Water hydration numbers within (A) 3.5 and (B) 6.5 Å from the cholesterol hydroxyl oxygen in DPPC (black), POPC (red), and DAPC (green) bilayers, which correspond to the first and second hydration shells, respectively. Membrane thickness along the cholesterol flip-flop path in DPPC (black), POPC (red), and DAPC (green) bilayers; the average thickness was calculated between (C) C2 carbons on the lipid glycerol backbone and between (D) C22/C32, the first methylene carbon atoms in both acyl chains.

Assuming that the interaction energy is similar to the enthalpic contribution to the PMFs, there must be a significant entropic contribution to compensate for the unfavorable interaction energy arising from desolvation penalty and reduction of favorable cholesterol−lipid interaction close to the bilayer center (Figures 3 and 4): $-T\Delta S \approx -8.8$ (DPPC), −9.9 (POPC), and −6.7 kcal/mol (DAPC). The favorable entropic contributions arise from the influence of the cholesterol orientation on the lipid chain packing and dynamics (along the path). To characterize this influence, we calculated the change of C−H order parameters ($|S_{CD}|$) along the path with respect to those in the minimum-PMF cholesterol orientation. The percent change of order parameters is defined as $\Delta S_{CD} = \Sigma_i (|S_{CD,i}| - |S_{CD,i}|_{min})/\Sigma_i |S_{CD,i}|_{min} \times 100$, where $|S_{CD,i}|$ and $|S_{CD,i}|_{min}$ are the order parameters from methylene carbons of all lipids at a cholesterol orientation (along the path) and the minimum-PMF orientation. As shown in Figure 6, the acyl chain order is decreased by ∼15% (DPPC), ∼13% (POPC), and ∼11% (DAPC) as the cholesterol moves toward the bilayer center. In fact, this reduction order is correlated with the reduction of favorable cholesterol−lipid interactions to the bilayer center (Figure 4); cholesterol with parallel orientations in the bilayer center makes the phospholipids more dynamic due to weaker interaction with cholesterol.

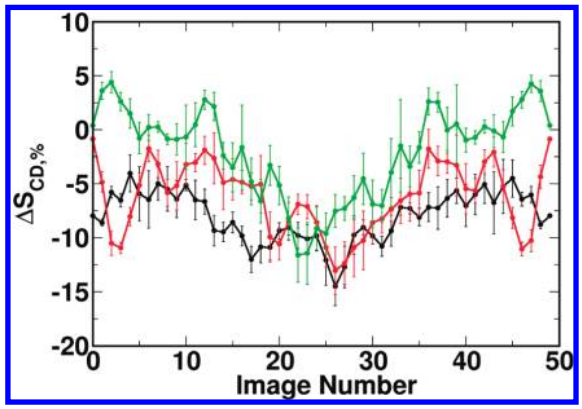

Figure 6. Average changes (ΔS_{CD}) of lipid order parameters along the path with respect to those in the PMF minimum orientation in DPPC (black), POPC (red), and DAPC (green) bilayers.

4. Conclusions

We have explored the energetics and mechanisms of cholesterol flip-flop using umbrella sampling and standard MD simulations in three different lipid bilayers: DPPC, POPC, and DAPC (Figure 1 and Supporting Information Figures S1−S3). The resulting 2D-PMFs as a function of the tilt angle (τ) of the rigid cholesterol ring and its center of mass along the *Z*-axis (Z_{CM}) show that the free energy minima for cholesterol in all three phospholipids are in an orientation with $\tau_{min} \approx 17-28°$ (Figure 2), which is consistent with the standard MD simulation results (Supporting Information Figure S8). A modified string method was used to calculate the most probable cholesterol flip-flop paths (Figures 2 and 3, Supporting Information Figures S5 and S6 and Supporting Information Movies M1−M3), and the resulting paths (Supporting Information Figure S9) indicate that cholesterol prefers to tilt first and move to the bilayer center where the free energy barrier exists. The free energy barriers near the bilayer center are 6.6 (DPPC), 7.0 (POPC), and 5.4 kcal/mol (DAPC) along the most probable flip-flop paths (Figure 3). Among the three lipid bilayers, DAPC has the lowest barrier for flip-flop. However, a free energy minimum does not exist at the bilayer center where cholesterol is parallel to the membrane surface, although such orientation was suggested by experiments and CG simulations.[8,10,35] It must be noted that the current umbrella sampling MD simulations were carried out in the lipid bilayers containing 2% mole fraction of cholesterol, meaning that the energy barrier of cholesterol flip-flop in the lipid bilayers containing 10% mole fraction of cholesterol used in experiments[8,35] could be different. However, the standard MD simulation with 10% mole fraction of cholesterol indicates similar results with umbrella sampling MD simulation regardless of the initial orientation of cholesterol (data not shown). Therefore, it appears that the concentration of cholesterol does not change the overall shape of the free energy barrier, suggesting that the C27r FF may require modifications to better represent the preference for parallel cholesterol at the center of poly-unsaturated lipid bilayers.[7,8] In addition, given the fact that the flip-flop rate in DAPC appears to be high even with the energy barrier in our calculations, it would be interesting to explore the cholesterol flip-flop rate in DAPC under conditions in which simulations can reproduce the experimental findings (i.e., a free energy minimum at the bilayer center), and to examine if the rate is consistent with the experimental data in the future. The current umbrella sampling scheme can be easily extended to explore cholesterol flip-flop events or other lipid phenomena in a biologically relevant bilayer having different lipid compositions in the inner and outer leaflets.

The present study also provides insights into the microscopic origin of the free energy barrier along the cholesterol flip-flop path in different levels of lipid acyl chain saturation. Interestingly, the decomposition of the total interaction energy into cholesterol−lipid and cholesterol−water interactions (Figure 4) indicates that the barrier of cholesterol−water interaction energy increases in the order of DPPC (8.5 kcal/mol), POPC (10.3 kcal/mol), and DAPC (11.4 kcal/mol). The desolvation penalty during cholesterol flip-flop is slightly more in unsaturated lipids because their membrane thickness is thinner (Figure 5). On the other hand, the reduction of favorable cholesterol−lipid interaction at the bilayer center is not significant in poly-unsaturated lipids, which significantly reduces the total interaction energy barrier of cholesterol flip-flop in poly-unsaturated lipids. Assuming that the interaction energy is similar to the enthalpic contribution to the PMFs, there must be a significant entropic contribution to compensate for the unfavorable interaction energy arising from desolvation penalty and reduction of favorable cholesterol−lipid interaction close to the bilayer center (Figure 3). The favorable entropic contributions arise from the influence of the cholesterol orientation on the lipid chain packing and dynamics along the path.

Acknowledgment. This work was supported by NSF Grant MCB-0918374 (to W.I.), institutional funding from the University of Maryland (J.B.K.), and a Howard Hughes Medical Institute Undergraduate Research Fellowship (J.B.L.). This research was also supported in part by NSF Grant OCI-0503992 through TeraGrid resources provided by Purdue University.

Supporting Information Available: Movies M1−M3 illustrating the evolution of the path in DPPC (M1), DOPC (M2), and DAPC (M3) in the modified MC-based string method, Table S1 showing detailed information about the simulation systems used in umbrella sampling simulations, Figures S1−S3 illustrating the restrained cholesterol orientations in umbrella sampling, Figure S4 showing the 2D-PMF up to 2 ns umbrella sampling, Figures S5 and S6 illustrating the pathway calculation, Figures S7 and S8 showing the time series of the cholesterol ring Z_{CM} and the probability distribution of the cholesterol tilt angle from the standard MD simulations, respectively, Figure S9 illustrating the cholesterol orientations along the most favorable flip-flop path in DPPC, Figure S10 showing the cholesterol orientation of the last snapshot from the standard MD simulations, and Figure S11 showing the histogram of the return time of cholesterols in standard MD simulations. This material is available free of charge via the Internet at http://pubs.acs.org.

References and Notes

(1) Scheidt, H. A.; Huster, D.; Gawrisch, K. Diffusion of cholesterol and its precursors in lipid membranes studied by H-1 pulsed field gradient magic angle spinning NMR. *Biophys. J.* **2005**, *89* (4), 2504–2512.

(2) Klauda, J. B.; Brooks, B. R.; Pastor, R. W. Dynamical Motions of Lipids and a Finite Size Effect in Simulations of Bilayers. *J. Chem. Phys.* **2006**, *125* (14), 144710.

(3) Zhang, Z.; Lu, L.; Berkowitz, M. L. Energetics of cholesterol transfer between lipid bilayers. *J. Phys. Chem. B* **2008**, *112*, 3807–3811.

(4) Sprong, H.; van der Sluijs, P.; van Meer, G. How proteins move lipids and lipids move proteins. *Nat. Rev. Mol. Cell Biol.* **2001**, *2* (7), 504–513.

(5) Mondal, M.; Mesmin, B.; Mukherjee, S.; Maxfield, F. R. Sterols are mainly in the cytoplasmic leaflet of the plasma membrane and the endocytic recycling compartment in CHO cells. *Mol. Biol. Cell* **2009**, *20* (2), 581–588.

(6) Fisher, K. A. Analysis of membrane halves: cholesterol. *Proc. Natl. Acad. Sci. U. S. A.* **1976**, *73* (1), 173–177.

(7) Harroun, T. A.; Katsaras, J.; Wassall, S. R. Cholesterol hydroxyl group is found to reside in the center of a polyunsaturated lipid membrane. *Biochemistry* **2006**, *45*, 1227–1233.

(8) Harroun, T. A.; Katsaras, J.; Wassall, S. R. Cholesterol is found to reside in the center of a polyunsaturated lipid membrane. *Biochemistry* **2008**, *47*, 7090–7096.

(9) Kučerka, N.; Marquardt, D.; Harroun, T. A.; Nieh, M.-P.; Wassall, S. R.; Katsaras, J. The functional significance of lipid diversity: Orientation of cholesterol in bilayers is determined by lipid species. *J. Am. Chem. Soc.* **2009**, *131*, 16358–16359.

(10) Marrink, S. J.; deVries, A. H.; Harroun, T. A.; Katsaras, J.; Wassall, S. R. Cholesterol shows preference for the interior of polyunsaturated lipid membranes. *J. Am. Chem. Soc.* **2008**, *130*, 10–11.

(11) Bennett, W. F. D.; MacCallum, J. L.; Hinner, M. J.; Marrink, S. J.; Tieleman, D. P. Molecular view of cholesterol flip-flop and chemical potential in different membrane environments. *J. Am. Chem. Soc.* **2009**, *131*, 12714–12720.

(12) Zhang, Z.; Lu, L.; Berkowitz, M. L. Energetics of cholesterol transfer between lipid bilayers. *J. Phys. Chem. B* **2008**, *112*, 3807–3811.

(13) Pan, A. C.; Sezer, D.; Roux, B. Finding transition pathways using the string method with swarms of trajectories. *J. Phys. Chem. B* **2008**, *112*, 3432–3440.

(14) Lee, J.; Im, W. Restraint potential and free energy decomposition formalism for helical tilting. *Chem. Phys. Lett.* **2007**, *441* (1−3), 132–135.

(15) Jo, S.; Lim, J. B.; Klauda, J. B.; Im, W. CHARMM-GUI Membrane Builder for mixed bilayers and its application to yeast membranes. *Biophys. J.* **2009**, *97* (1), 50–58.

(16) Jo, S.; Kim, T.; Im, W. Automated builder and database of protein/membrane complexes for molecular dynamics simulations. *PLos ONE* **2007**, *2* (9), e880.

(17) Jo, S.; Kim, T.; Iyer, V. G.; Im, W. CHARMM-GUI: A web-based graphical user interface for CHARMM. *J. Comput. Chem.* **2008**, *29* (11), 1859–1865.

(18) Klauda, J. B.; Kucerka, N.; Brooks, B. R.; Pastor, R. W.; Nagle, J. F. Simulation-based methods for interpreting X-ray data from lipid bilayers. *Biophys. J.* **2006**, *90* (8), 2796–2807.

(19) Skibinsky, A.; Venable, R. M.; Pastor, R. W. A molecular dynamics study of the response of lipid bilayers and monolayers to trehalose. *Biophys. J.* **2005**, *89* (6), 4111–4121.

(20) Brooks, B. R.; Brooks, C. L.; Mackerell, A. D.; Nilsson, L.; Petrella, R. J.; Roux, B.; Won, Y.; Archontis, G.; Bartels, C.; Boresch, S.; Caflisch, A.; Caves, L.; Cui, Q.; Dinner, A. R.; Feig, M.; Fischer, S.; Gao, J.; Hodoscek, M.; Im, W.; Kuczera, K.; Lazaridis, T.; Ma, J.; Ovchinnikov, V.; Paci, E.; Pastor, R. W.; Post, C. B.; Pu, J. Z.; Schaefer, M.; Tidor, B.; Venable, R. M.; Woodcock, H. L.; Wu, X.; Yang, W.; York, D. M.; Karplus, M. CHARMM: The biomolecular simulation program. *J. Comput. Chem.* **2009**, *30* (10), 1545–1614.

(21) Klauda, J. B.; Brooks, B. R.; MacKerell, A. D.; Venable, R. M.; Pastor, R. W. An ab initio study on the torsional surface of alkanes and its effect on molecular simulations of alkanes and a DPPC bilayer. *J. Phys. Chem. B* **2005**, *109*, 5300–5311.

(22) Klauda, J. B.; Pastor, R. W.; Brooks, B. R. Adjacent gauche stabilization in linear alkanes: Implications for polymer models and conformational analysis. *J. Phys. Chem. B* **2005**, *109*, 15684–15686.

(23) Durell, S. R.; Brooks, B. R.; Bennaim, A. Solvent-induced forces between two hydrophilic groups. *J. Phys. Chem.* **1994**, *98*, 2198–2202.

(24) Jorgensen, W. L.; Chandrasekhar, J.; Madura, J. D.; Impey, R. W.; Klein, M. L. Comparison of simple potential functions for simulating liquid water. *J. Chem. Phys.* **1983**, *79* (2), 926–935.

(25) Ryckaert, J. P.; Ciccotti, G.; Berendsen, H. J. C. Numerical-integration of Cartesian equations of motion of a system with constraints—Molecular-dynamics of N-alkanes. *J. Comput. Phys.* **1977**, *23* (3), 327–341.

(26) Brooks, C. L., III; Pettitt, B. M.; Martin, K. Structural and energetic effects of truncating long ranged interactions in ionic and polar fluids. *J. Chem. Phys.* **1985**, *83* (11), 5897–5908.

(27) Steinbach, P. J.; Brooks, B. R. New spherical-cutoff methods for long-range forces in macromolecular simulation. *J. Comput. Chem.* **1994**, *15* (7), 667–683.

(28) Essmann, U.; Perera, L.; Berkowitz, M. L.; Darden, T.; Lee, H.; Pedersen, L. G. A smooth particle mesh Ewald potential. *J. Chem. Phys.* **1995**, *103*, 8577–8592.

(29) Kumar, S.; Bouzida, D.; Swendsen, R. H.; Kollman, P. A.; Rosenberg, J. M. The weighted histogram analysis method for free-energy calculations on biomolecules. 1. The method. *J. Comput. Chem.* **1992**, *13* (8), 1011–1021.

(30) Metropolis, N.; Ulam, S. The Monte Carlo method. *J. Am. Stat. Assoc.* **1949**, *44* (247), 335–341.

(31) Klauda, J. B.; Brooks, B. R.; MacKerell, A. D., Jr.; Venable, R. M.; Pastor, R. W. An ab initio study on the torsional surface of alkanes and its effect on molecular simulations of alkanes and a DPPC bilayer. *J. Phys. Chem. B* **2005**, *109*, 5300–5311.

(32) Backer, J. M.; Dawidowicz, E. A. The rapid transmembrane movement of cholesterol in small unilamellar vesicles. *Biochim. Biophys. Acta* **1979**, *551* (2), 260–270.

(33) Leventis, R.; Silvius, J. R. Use of cyclodextrins to monitor transbilayer movement and differential lipid affinities of cholesterol. *Biophys. J.* **2001**, *81* (4), 2257–2267.

(34) Steck, T. L.; Ye, J.; Lange, Y. Probing red cell membrane cholesterol movement with cyclodextrin. *Biophys. J.* **2002**, *83* (4), 2118–2125.

(35) Shaikh, S. R.; Cherezov, V.; Caffrey, M.; Soni, S. P.; LoCascio, D.; Stillwell, W.; Wassall, S. R. Molecular organization of cholesterol in unsaturated phosphatidylethanolamines: X-ray diffraction and solid state H-2 NMR reveal differences with phosphatidylcholines. *J. Am. Chem. Soc.* **2006**, *128*, 5375–5383.

JP108166K